American Mineralogist, Volume 67, pages 69–75, 1982

Crystal structure of a pink muscovite from Archer's Post, Kenya: implications for reverse pleochroism in dioctahedral micas

STEVEN M. RICHARDSON

Department of Earth Sciences, Iowa State University

AND JAMES W. RICHARDSON, JR.

Department of Chemistry, Iowa State University and U.S. DOE Ames Research Laboratory, Ames, Iowa 50011

Abstract

The crystal structure of a reverse pleochroic muscovite containing both Fe^{3+} and Mn^{3+} has been determined by standard single-crystal X-ray methods. The mica has a $2M_1$ polytype, space group $C\,2/c$. Cell constants are $a = 5.1988$Å *esd* 0.0021, $b = 9.0266$Å *esd* 0.0019, $c = 20.1058$Å *esd* 0.0044, $\beta = 95.782°$ *esd* 0.039, $V = 938.72$Å *esd* 0.48. Average bond lengths in tetrahedral sites are 1.646Å and 1.639Å, comparable to bond lengths in Si–Al tetrahedra of other analyzed muscovites, but also compatible with minor site occupancy by Fe^{3+}. Mean bond strengths and electron densities for the sites are also compatible with but do not require minor amounts of tetrahedral Fe^{3+}. A pleochroic mechanism related to tetrahedral Fe^{3+}, therefore, cannot be ruled out. Thermal vibration ellipsoids of atoms in the octahedral layer, however, are oriented with long axes perpendicular to the layer, which suggests the possibility that reverse pleochroism is due instead to an unusual configuration of d-orbitals for octahedrally-coordinated Fe^{3+} or Mn^{3+}.

Introduction

The pink muscovite from Archer's Post, Kenya, was first chemically analyzed and described by Richardson (1975), hereafter referred to as "paper I." The chemical analysis from that study is reproduced in Table 1. Mössbauer and optical absorption spectroscopy were used to relate optical properties of the mica to its crystal chemistry. The Archer's Post muscovite is reversely pleochroic; that is, it absorbs polarized light more efficiently when that light is vibrating in a plane perpendicular to the basal cleavage [E ⊥ (001)] than when it is parallel to it [E ∥ (001)]. Trioctahedral micas are occasionally reversely pleochroic, but the Archer's Post muscovite is still the only reported example of reverse pleochroism in a dioctahedral mica.[1]

Spectra recorded in paper I were ambiguous but generally supported the conclusion that reverse pleochroism is the result of charge transfer between a tetrahedrally-coordinated Fe^{3+} ion and an O^{2-} ligand that bridges to the layer of octahedrally-coordinated cations. Absorption is enhanced when the electric vector of the polarized light beam is coupled with the vibronic mode of the Fe^{3+}–O^{2-} bond, which is roughly parallel to [001]. This mechanism was first suggested for trioctahedral micas (Faye and Hogarth, 1969; Hogarth *et al.*, 1970), and it was reasonable to expect it to apply to dioctahedral micas as well.

Shortly after paper I appeared, however, Annersten and Hålenius (1976) published a critique which questions the likelihood of Fe^{3+} in tetrahedral coordination. They compared spectra in paper I with their own and with one recorded for a ferrian muscovite by Goodman (1976) and concluded that Fe^{3+} is almost certainly in octahedral coordination in the Archer's Post muscovite. This conclusion poses a dilemma, expressed by Richardson (1976): either "(1) Annersten and Hålenius are correct, and Faye and Hogarth's explanation does not apply to reverse pleochroic dioctahedral micas or (2) Faye and Hogarth's mechanism applies to reverse pleochroic muscovite, and Annersten and Hålenius are wrong." The work that is the subject of this paper

[1]Paper I reports that a rose muscovite from Pilar, N. M. (Schaller and Henderson, 1926) is also reversely pleochroic. Gresens and Stensrud (1977), however, have pointed out that this statement was the result of a misreading of Schaller and Henderson's paper.

0003–004X/82/0102–0069$02.00

Table 1. Chemical composition of the Archer's Post Muscovite in weight percent (from Richardson, 1975)

SiO_2	45.1
Al_2O_3	34.60
TiO_2	0.56
Fe_2O_3	2.81
FeO	<0.1
Mn_2O_3	0.55
MgO	0.64
CaO	0.1
BaO	0.09
ZnO	0.01
Na_2O	0.21
K_2O	10.4
Rb_2O	<0.01
H_2O^+	4.85
Total	99.94

was undertaken to resolve that dilemma by using single-crystal X-ray diffraction methods to examine the structure of the Archer's Post mica and to analyze the geometry of possible sites for Fe^{3+}.

Experimental methods

In the geological environment at Archer's Post, all of the muscovite appears to have suffered at least mild mechanical stresses. As a result, perfectly flat mica flakes are not available for study. Considerable efforts were made, however, to find a crystal in which distortions were minimal.

Several large flakes of mica, free of optically resolvable inclusions, were cooled in acetone and dry ice and were crushed gently in an agate mortar to produce cleavage fragments roughly 50 to 500 μm across. These were hand sorted under a polarizing microscope to select grains which were optically homogeneous and untwinned and which had a maximum dimension less than 100 μm. More than twenty of these were mounted on glass fibers and examined with oscillation photographs before one was found that was free of gross mechanical distortion, as revealed by the smearing or doubling of reflections.

Diffraction intensities were measured at room temperature on a four-circle diffractometer, automated with a PDP-15 computer under the control of the data collection program ALICE (Jacobson, 1974). Data were gathered using Mo$K\alpha$ radiation (λ = 0.71034Å) monochromatized by a flat graphite crystal. A provisional reduced cell was calculated on the basis of twelve indexed reflections, and the angular settings on the instrument were referenced to that cell for all subsequent operations.

Reflections were collected in the octants (hkl), $(\bar{h}k\bar{l})$, $(\bar{h}\bar{k}l)$, and $(h\bar{k}\bar{l})$ in the range $2° < 2\theta < 60°$. Background intensities were measured on both sides of each peak, averaged, and subtracted from the integrated intensity to obtain the final intensity data. During data collection, peaks with intensities less than zero or for which I(obs) was less than three times the standard deviation of intensities were flagged for later deletion from the data set. After 1200 reflections had been measured, it was apparent that those with $h + k \neq 2n$ were systematically extinct, indicating a C-centered Bravais lattice. The remaining reflections were, therefore, collected under that constraint. Intensities and positions of three standard reflections were checked after each 30 data points. No decay of counting intensities was observed. Altogether 3892 reflections were measured.

Due to its pronounced basal cleavage, the crystal fragment chosen for study departed dramatically from spherical geometry. An empirical correction for absorption was, therefore, computed for each reflection. The technique, described by Karcher (1981), is based on the method of North *et al.* (1968) and has been used successfully in a large number of structure determinations in this laboratory. To derive the absorption function, intensities were measured in 10° intervals in ϕ on a strong reflection with its reciprocal lattice vector parallel to the ϕ axis of the goniometer ($\chi = 90°$). These measurements are used to approximate the variance in transmittance with ϕ. In many cases, this absorption correction has been shown to be better than analytical results based on measured crystal dimensions. Standard corrections for Lorentz and polarization effects were also performed.

All reflections marked as absent or statistically questionable during data collection were removed from the set at the beginning of data reduction. The remaining list of 1884 data points was searched for symmetrically equivalent reflections. Their intensities were averaged and regrouped to form a list of independent reflections. The final list, minus a small set of reflections for which $|F(obs) - F(ave)| > 6.0\sigma_F$, contained 879 reflections. The set of F(obs) and F(calc) values for these reflections is shown in Table 2.[2]

[2]To receive a copy of Table 2, order Document AM-82-185 from the Business Office, Mineralogical Society of America, 2000 Florida Avenue, N.W., Washington, D. C. 20009. Please remit $1.00 in advance for the microfiche.

In paper I the Archer's Post muscovite was identified as a $2M_1$ mica on the basis of the orientation of percussion figures relative to the optic axial plane. The space group for a $2M_1$ polytype is $C\,2/c$, consistent with the observed systematic extinctions. Statistical tests were performed on the complete set of intensity data to verify that the unit cell is centrosymmetric, ruling out the space group Cc, which has the same extinction criteria. X-ray data, therefore, confirm the earlier determination.

Twelve cycles of full-matrix least squares refinement were performed on the data, using the program ALLS (Lapp and Jacobson, 1979). Atomic position parameters for the initial cycle were those of Radoslovich (1962). To simplify calculation, the two tetrahedrally-coordinated sites were each initially assumed to be completely filled with silicon and the octahedrally-coordinated site with aluminum. Atomic scattering factors were chosen accordingly, using values tabulated in the *International Tables for X-ray Crystallography* (1962). The errors introduced by these assumptions are probably small, since Si^{4+} and Al^{3+} are the major cations in these sites, and impurity ions are either low in abundance or similar in atomic number (Table 1).

After six cycles of refinement, anisotropic thermal vibration parameters were allowed to vary for all atoms, and a scaling constant on scattering factors (*m* in Table 3) was allowed to vary for all cation sites. After another three cycles, weighting factors were introduced in the intensity data to correct for the uneven distribution of reflections measured over the range of 2θ values. Progress of the refinement was checked after every third cycle by generating a difference map based on measured and calculated electron densities. The final cell dimensions, scattering factor scaling constants, atomic position parameters, and anisotropic thermal vibration parameters are reported in Table 3. The value of R(unweighted) is 0.099, and R(weighted) is 0.129. These compare favorably with the residual index for the raw data ($R = \Sigma||F(obs)| - |F(ave)||/\Sigma|F(ave)| = 0.084$), which sets an absolute lower limit for the refinement. Considering the difficulties encountered in selecting the crystal used for this study, it is unlikely that a substantial improvement could be made in these values.

Table 3. Atomic site parameters

	K	Si-A	Si-B	Al	O-A
m	0.922(22)	0.956(20)	0.946(20)	1.001(22)	1.0
x	0.0	0.4510(5)	0.0354(5)	0.2506(5)	0.3872(14)
y	0.0992(4)	0.2587(3)	0.4298(3)	0.0838(3)	0.2525(7)
z	0.25	0.1355(1)	0.3646(1)	0.0002(1)	0.0543(3)
$*\beta_{11}$	188.8(18)	114.8(11)	99.6(9)	73.2(7)	172.9(16)
$*\beta_{22}$	84.3(3)	47.1(1)	50.6(2)	45.1(1)	68.2(2)
$*\beta_{33}$	19.87(1)	15.04(1)	14.14(1)	13.04(1)	16.55(1)
$*\beta_{12}$	0.0	-4.62(2)	-10.43(6)	0.13(0)	-10.48(6)
$*\beta_{13}$	9.21(2)	8.07(2)	5.60(1)	2.47(1)	12.35(3)
$*\beta_{23}$	0.0	1.52(0)	-1.47(0)	2.31(0)	0.45(0)

	O-B	O-C	O-D	O-E	OH
m	1.0	1.0	1.0	1.0	1.0
x	0.0366(13)	0.4178(15)	0.2475(13)	0.2509(14)	0.0422(14)
y	0.4431(8)	0.0931(8)	0.3712(8)	0.3132(9)	0.0622(8)
z	0.4459(3)	0.1685(4)	0.1685(4)	0.3424(4)	0.4492(4)
$*\beta_{11}$	159.4(15)	257.2(24)	154.0(14)	196.1(18)	195.6(18)
$*\beta_{22}$	65.9(2)	83.9(3)	87.8(3)	95.0(3)	81.4(3)
$*\beta_{33}$	17.11(1)	17.21(1)	19.82(1)	22.56(1)	18.31(1)
$*\beta_{12}$	16.23(9)	4.33(2)	16.93(9)	9.27(5)	-17.61(9)
$*\beta_{13}$	3.26(1)	11.94(3)	4.07(1)	4.05(1)	10.37(3)
$*\beta_{23}$	7.51(1)	0.83(0)	3.10(0)	-6.89(1)	1.20(0)

*Coefficients in the expression $\exp-(\beta_{11}h^2+\beta_{22}k^2+\beta_{33}l^2+2\beta_{12}hk+2\beta_{13}hl+2\beta_{23}kl)$, multiplied by 10^4. Parenthesized figures represent estimated standard deviations (esd). These indicate the uncertainty in the smallest units shown for a tabulated value.

Discussion

Distances and angles between ions in polyhedral units have long been recognized as a measure of site occupancy (*e.g.*, Smith, 1954). Calculated interatomic distances and selected interatomic angles for each of the four cation sites in the refined structure are tabulated in Table 4. A slight difference in the average cation–oxygen bond lengths for the "Si"–A and "Si"–B tetrahedra may indicate ordering on the two sites, in agreement with Radoslovich (1962) but contrary to the results of Güven (1967) and Rothbauer (1971).

It is difficult to separate the effects of Fe^{3+} and Al^{3+} on tetrahedral dimensions from each other. Empirically, since ionic radii increase in the order $Si^{4+} < Al^{3+} < Fe^{3+}$ (Shannon and Prewitt, 1969), the substitution of a small amount of Fe^{3+} for Si^{4+} should have the same effect on mean bond length as the substitution of a somewhat larger amount of Al^{3+}. Table 5 contains mean tetrahedral bond lengths, abstracted from published reports, for a number of mica structures with varying amounts of Al^{3+} and Fe^{3+} in tetrahedral substitution. The data of Steinfink (1962), Donnay *et al.* (1964a), Steadman and Nuttall (1963), and Bailey (1975) can be used to define a linear relationship between $Fe^{3+}/(Fe^{3+} + Si^{4+})$ and mean bond length that can be applied to the data in Table 4. The resulting inferred site occupancy is meaningless, though, since any number of linear relationships involving

Table 4. Selected interatomic distances and angles

K site:			
K-O(C)$_1$	2.850(8)Å		
K-O(D)$_1$	2.865(8)Å		
K-O(E)$_1$	2.897(8)Å		
K-O(C)$_2$	3.294(8)Å		
K-O(D)$_2$	3.285(8)Å		
K-O(E)$_2$	3.504(9)Å		
"Si"-A site:			
Si(A)-O(A)	1.634(7)Å	O(A)-Si(A)-O(C)	110.57(38)°
Si(A)-O(C)	1.652(8)Å	O(A)-Si(A)-O(D)	110.41(38)°
Si(A)-O(D)	1.653(8)Å	O(A)-Si(A)-O(E)	111.82(40)°
Si(A)-O(E)	1.644(8)Å	O(C)-Si(A)-O(D)	107.31(40)°
mean	1.646(8)Å	O(C)-Si(A)-O(E)	107.21(42)°
		O(D)-Si(A)-O(E)	109.36(41)°
"Si"-B site:			
Si(B)-O(B)	1.639(7)Å	O(B)-Si(B)-O(C)	110.55(39)°
Si(B)-O(C)	1.645(8)Å	O(B)-Si(B)-O(D)	110.04(38)°
Si(B)-O(D)	1.640(7)Å	O(B)-Si(B)-O(E)	112.81(40)°
Si(B)-O(E)	1.632(8)Å	O(C)-Si(B)-O(D)	106.73(41)°
mean	1.639(8)Å	O(C)-Si(B)-O(E)	109.46(42)°
		O(D)-Si(B)-O(E)	107.02(41)°
"Al" site:			
Al-O(A)$_1$	1.962(7)Å	O(A)$_1$-Al-O(A)$_2$	79.25(33)°
Al-O(A)$_2$	1.933(7)Å	O(A)$_1$-Al-O(B)$_1$	98.87(31)°
Al-O(B)$_1$	1.946(7)Å	O(A)$_1$-Al-O(B)$_2$	92.46(31)°
Al-O(B)$_2$	1.940(7)Å	O(A)$_1$-Al-OH$_2$	92.69(32)°
Al-OH$_1$	1.933(8)Å	O(A)$_2$-Al-O(B)$_1$	92.29(31)°
Al-OH$_2$	1.924(8)Å	O(A)$_2$-Al-OH$_4$	93.77(32)°
		O(A)$_2$-Al-OH$_2$	96.25(32)°
		O(B)$_1$-Al-O(B)$_2$	78.80(32)°
		O(B)$_1$-Al-OH$_1$	92.08(32)°
		O(B)$_2$-Al-OH$_1$	96.20(32)°
		O(B)$_2$-Al-OH$_2$	94.32(32)°
		OH$_1$-Al-OH$_2$	77.29(35)°

Parenthesized figures represent estimated standard deviations (esd). These indicate the uncertainty in the smallest units shown for a tabulated value.

the ions Si^{4+}, Al^{3+}, and Fe^{3+} could be devised to arrive at different inferred site occupancy values. The best this approach can provide is a maximum figure for Fe^{3+} substitution of about 4 percent.

The bond strength–bond length curves of Brown and Shannon (1973) present no more conclusive means of testing site occupancy here because the amount of Fe^{3+} available for substitution in the tetrahedral sites is only equivalent to 3.5 percent of the total site occupancy, according to the chemical analysis in Table 1. Total bond strengths for each of the tetrahedral sites have been calculated using the alternative assumptions that the sites contain 25% Al^{3+} or 21.5% Al^{3+} and 3.5% Fe^{3+}. In each case, the bond strength calculated assuming that Fe^{3+} is present is closer to the ideal 4.0 but is within the limit of error for the calculation performed assuming substitution by Al^{3+} alone.

A third approach, based not on bond lengths but on the refined values of the scattering factor scaling constant (m, Table 3), also yields ambiguous results. The final values for both tetrahedral sites are less than 1.0, which indicates that the average ion on those sites has a composite scattering factor slightly less than that for a Si^{4+} ion, an anticipated effect of Al^{3+} substitution. If we assume that the tetrahedral sites are each fully occupied and that only Si^{4+} and Al^{3+} are present, we can calculate a theoretical minimum value for m of 0.982. A maximum (m = 1.015) can be calculated by assuming that all of the Fe^{3+} in the chemical analysis replaces Al^{3+} in the two sites. Since both the minimum and the maximum lie within 3σ of the m values in Table 3, however, the site occupancies are again indeterminate, though the values in Table 3 are low enough to suggest that the Fe^{3+} content of both sites is minimal.

In short, the data do not provide a basis for an unambiguous answer to the question: "Is reverse pleochroism in this muscovite due to tetrahedrally coordinated Fe^{3+}?" Other features of the structure, however, support a possible alternative. Figure 1a is a perspective drawing of a portion of the Archer's Post muscovite structure, centered on the octahedrally-coordinated cation layer. For comparison, the same portion of a muscovite structure investigated by Rothbauer (1971) is shown in Figure 1b. The thermal vibration ellipsoids for the "Al" cations and for the oxygens O–A, O–B, and OH, to which they are bonded, have their major axes oriented roughly perpendicular to the octahedral layer in the Archer's Post structure. This is in marked contrast to Rothbauer's structure, in which thermal vibration ellipsoids for these ions are oriented with their long axes in the plane of the layer.

Table 5. Mean tetrahedral bond lengths from selected mica structures

Mineral	Bond length	Reference
Muscovite (Al_2Si_2)	1.69(5)Å	Radoslovich (1962)
(Si_4)	1.61(2)Å	
Muscovite ($AlSi_3$)	1.643(2)Å	Güven (1967)
($AlSi_3$)	1.643(2)Å	
Muscovite ($AlSi_3$)	1.645(2)Å	Rothbauer (1971)
($AlSi_3$)	1.644(2)Å	
Phlogopite ($FeSi_3$)	1.681(20)Å	Steinfink (1962)
Ferriannite ($FeSi_3$)	1.685(11)Å	Donnay et al. (1964a)
Cronstedtite-1H (Fe_2Si_2)	1.73Å	Steadman and Nuttall (1963)
Cronstedtite-2H$_2$ (Fe_4)	1.801Å	Bailey (1975)
(Si_4)	1.617Å	

The estimated standard deviations of the orthogonal atomic position coordinates (X, Y, Z) of the "Al" cation are 0.00256Å, 0.00278Å, and 0.00280Å, respectively, indicating that the shape and orientation of its ellipsoid are, in fact, functions of anisotropic thermal motion rather than uncertainties of measurement. It is intriguing to notice that the ellipsoids are oriented parallel to the direction of maximum light absorption.

The orientation of these thermal vibration ellipsoids could be an artifact generated by our absorption correction technique. We feel that this is unlikely, however. The absorption correction technique has been applied successfully to data from many plate-like crystals in this laboratory and has never previously had this effect. Furthermore, the ellipsoid orientations in this mica are not uniform across the structure. The perpendicular orientation is strongest within the octahedral layer, and does not extend to the interlayer potassium ions. We consider the observed orientations, therefore, to be real.

Burns (1970, p. 67) has pointed out that pleochroism often occurs when transition metal ions are placed in low-symmetry sites, and it is well-recognized that the octahedrally coordinated sites in mica are usually distorted as a means of making octahedral and tetrahedral sheet dimensions compatible (*e.g.*, Donnay *et al.*, 1964b). The bond angle deviation,

$$\sigma\ (\text{oct}) = \frac{1}{11}\sum_{i=1}^{12}(\theta_i - 90°)^2,$$

(Robinson *et al.*, 1971) for the octahedral unit in Rothbauer's structure, for example, is 7.68°. The mean square bond length deviation,

$$\Delta(\text{oct}) = \frac{1}{6}\sum_{i=1}^{6}[(l_i - \bar{l})/\bar{l}]^2,$$

(Brown and Shannon, 1973) for the same structure, another measure of distortion, is 0.000034Å^2. For the Archer's Post mica structure, these two values are 7.47° and 0.000039Å^2, respectively. Octahedrally-coordinated sites in the Archer's Post structure, therefore, are distorted to approximately the same degree as those in Rothbauer's structure, presumably of a normally pleochroic muscovite. The difference between the two, as indicated by the thermal ellipsoid orientations, is the direction, rather than the amount of distortion. Whether this difference can account for the reverse pleochroism in the Archer's Post sample is less certain.

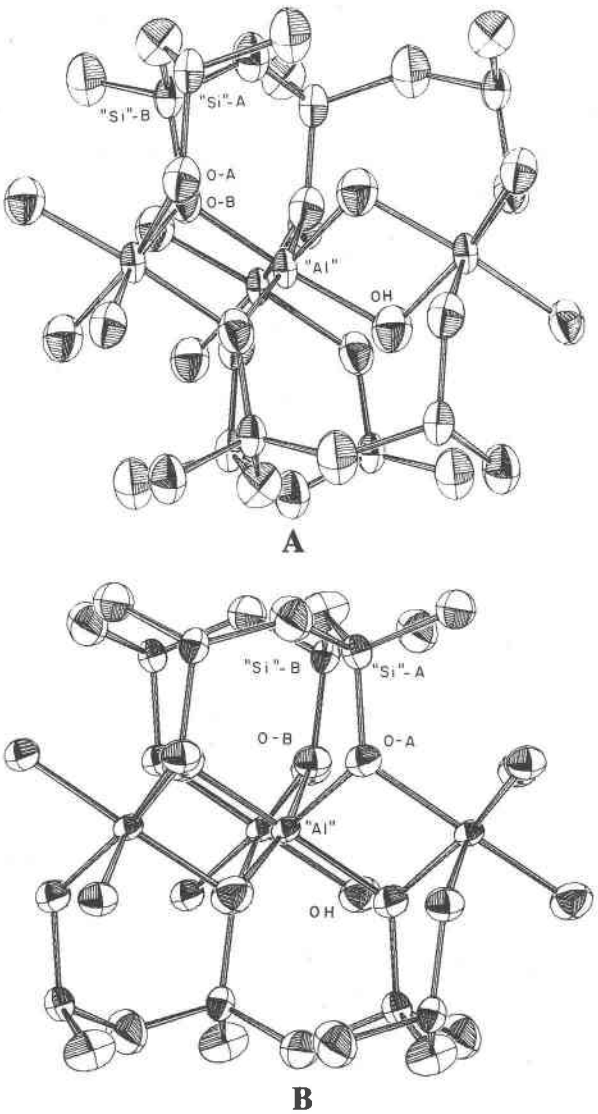

Fig. 1: Perspective drawings of a portion of the muscovite structure, centered on the octahedrally coordinated "Al" layer, prepared using the plotting program ORTEP (Johnson, 1965). (a) The Archer's Post mica structure. Thermal vibration ellipsoids represent the 70% probability electron distribution surface. (b) The muscovite structure reported by Rothbauer (1971). Thermal vibration ellipsoids represent the 95% probability electron distribution surface.

One possible effect of the ellipsoid orientation might be to weaken the mechanism currently understood to enhance normal pleochroism in micas. Charge transfer between transition metal ions in adjacent octahedral sites (for example, $Fe^{2+} \rightarrow Fe^{3+}$) accounts for a strong absorption in the UV and in short visible wavelengths of light. Such charge transfer occurs most readily when light is polarized in the plane of the octahedral sheet (Faye,

1968; Robbins and Strens, 1972). In biotite, the pleochroic effect is particularly strong because the crystallographically distinct M1 and M2 octahedral sites are both filled and may have different proportions of transition metals in them. As Goodman (1976) has shown, however, the M2 site in muscovite is occupied only under unusual conditions, when there is an excess of metal ions above that necessary to fill the M1 site. This is not the case for the Archer's Post sample, for which no residual electron density is associated with the M2 site. Furthermore, iron and manganese in the Archer's Post mica are assumed to be present only in the 3+ oxidation state (paper I), so that charge transfer is not possible between transition metal ions in the occupied sites. Even if this were not so, however, the prominent orientation of the thermal ellipsoids suggests a minimized overlap of valence electron fields in the octahedral layer. If so, this would also weaken the charge transfer mechanism.

Although the charge transfer mechanism discussed above is responsible for much of the normal pleochroic scheme, the visible absorption spectrum is dominated by relatively weak spin forbidden d–d bands. In paper I, much of the visible absorption was attributed to d–d transitions in Mn^{3+}. Annersten and Hålenius (1976) and Goodman (1976) present compelling evidence that most of the remaining bands are due to transitions in octahedrally coordinated Fe^{3+}. Faye (1968) suggests similar band assignments and considers the possibility that some energy levels of octahedrally coordinated Fe^{3+} that are subject to Jahn–Teller splitting may account for features in the violet and near UV wavelength range, particularly if the site is distorted from O_h symmetry. It is possible, if the d-orbitals of Fe^{3+} and Mn^{3+} are influenced by the orientation of the thermal vibration ellipsoids, that some of these absorption bands may be deeper for light polarized perpendicular to the octahedral layer than for light polarized parallel to it, resulting in a reversed pleochroic scheme.

Conclusions

The structure refinement undertaken in this study has been unable to verify or to rule out the presence of Fe^{3+} in tetrahedrally-coordinated sites of the Archer's Post muscovite. For the small amount of iron involved, standard means of estimating site occupancy with X-ray data and crystal chemical arguments are not sensitive enough to serve as diagnostic tools. On the other hand, examination of the octahedrally-coordinated sites shows that the orientation of thermal vibration ellipsoids differs from that in a "normal" muscovite and is roughly parallel to the direction of maximum light absorption by the sample. Whether this orientation can be used as the basis for an alternative explanation for reverse pleochroism in the mica depends on two factors: (1) the coupling of valence electron fields of the octahedrally coordinated cations with the thermal motion described by the ellipsoids and (2) the extent to which that coupling may be effective at altering the energy levels of d-electrons associated with orbitals lying in or perpendicular to the octahedral layer. Neither is easy to demonstrate. In the absence of such an alternative mechanism, however, the explanation for reverse pleochroism given by Faye and Hogarth (1969) is still the only plausible one, despite the conflicting spectroscopic data.

Acknowledgments

The authors are grateful to Robert A. Jacobson, DOE Ames Research Laboratory, for the use of his equipment and computing facilities, as well as for helpful suggestions during this project. R. Benson and B. Karcher also provided valuable assistance. Computer funds were also provided by the Department of Earth Sciences, Iowa State University. This manuscript has benefitted from critical reviews by R. A. Jacobson, R. Hazen, R. G. Burns, and D. D. Hogarth.

References

Annersten, H. and Hålenius, U. (1976) Ion distribution in pink muscovite: a discussion. American Mineralogist, 61, 1045–1050.

Bailey, S. W. (1975) Cation ordering and pseudosymmetry in layer silicates. American Mineralogist, 60, 175–187.

Brown, I. D. and Shannon, R. D. (1973) Empirical bond-strength–bond-length curves for oxides. Acta Crystallographica, A29, 266–282.

Burns, R. G. (1970) Mineralogical Applications of Crystal Field Theory. Cambridge University Press, Cambridge, Great Britain.

Donnay, G., Morimoto, N., Takeda, H., and Donnay, J. D. H. (1964a) Trioctahedral one-layer micas. I. Crystal structure of a synthetic iron mica. Acta Crystallographica, 17, 1369–1372.

Donnay, G., Donnay, J. D. H., and Takeda, H. (1964b) Trioctahedral one-layer micas. II. Prediction of the structure from composition and cell dimensions. Acta Crystallographica, 17, 1374–1381.

Faye, G. H. (1968) The optical absorption spectra of certain transition metal ions in muscovite, lepidolite, and fuchsite. Canadian Journal of Earth Sciences, 5, 31–38.

Faye, G. H. and Hogarth, D. D. (1969) On the origin of "reverse" pleochroism of a phlogopite. Canadian Mineralogist, 10, 25–34.

Goodman, B. A. (1976) The Mössbauer spectrum of a ferrian muscovite and its implications in the assignment of sites in dioctahedral micas. Mineralogical Magazine, 40, 513–518.

Gresens, R. L. and Stensrud, H. L. (1977) More data on red muscovite. American Mineralogist, 62, 1245–1251.

Güven, N. (1967) The crystal structures of $2M_1$ phengite and $2M_1$ muscovite. Carnagie Institute of Washington Yearbook, 66, 487–492.

Hogarth, D. D., Brown, F. F., and Pritchard, A. M. (1970) Biabsorption, Mössbauer spectra, and chemical investigation of five phlogopite samples from Quebec. Canadian Mineralogist, 10, 710–722.

International Tables for X-Ray Crystallography (1962) C. H. MacGillavry and G. D. Rieck, eds., Kynoch Press, Birmingham, England.

Jacobson, R. A. (1974) An algorithm for automatic indexing and Bravais lattice selection: the programs BLIND and ALICE. U.S. National Technical Information Service, IS-3469.

Johnson, C. K. (1965) A FORTRAN thermal ellipsoid plot program for crystal structure illustrations. U.S. National Technical Information Service, ORNL-3794.

Karcher, B. A. (1981) The crystal and molecular structures of selected organic and organometallic compounds and an algorithm for empirical absorption correction. Ph.D. Thesis, Iowa State University, Ames.

Lapp, R. L. and Jacobson, R. A. (1979) ALLS, a generalized crystallographic least squares program. U.S. National Technical Information Service, IS-4708.

North, A. C. T., Phillips, D. C., and Mathews, F. S. (1968) A semi-empirical method of absorption correction. Acta Crystallographica, A24, 351–359.

Radoslovich, E. W. (1962) The structure of muscovite, $KAl_2(Si_3Al)O_{10}(OH)_2$. Acta Crystallographica, 13, 919–932.

Richardson, S. M. (1975) A pink muscovite with reverse pleochroism from Archer's Post, Kenya. American Mineralogist, 60, 73–78.

Richardson, S. M. (1976) Ion distribution in pink muscovite: a reply. American Mineralogist, 61, 1051–1052.

Robbins, D. W. and Strens, R. G. J. (1972) Charge-transfer in ferromagnesian silicates: The polarized electronic spectra of trioctahedral micas. Mineralogical Magazine, 38, 551–563.

Robinson, K., Gibbs, G. V., and Ribbe, P. H. (1971) Quadratic elongation: a quantitative measure of distortion in coordination polyhedra. Science, 172, 567–570.

Rothbauer, R. (1971) Untersuchung eines $2M_1$-Muscovits mit Neutronenstrahlen. Neues Jahrbuch für Mineralogie, Monatshefte, 1971, 143–154.

Schaller, W. T. and Henderson, E. P. (1926) Purple muscovite from New Mexico. American Mineralogist, 11, 5–16.

Shannon, R. D. and Prewitt, C. T. (1969) Effective ionic radii in oxides and fluorides. Acta Crystallographica, B25, 925–946.

Smith, J. V. (1954) A review of Al–O and Si–O distances. Acta Crystallographica, 7, 479–481.

Steadman, R. and Nuttall, P. M. (1963) Polymorphism in cronstedtite, Acta Crystallographica, 16, 1–8.

Steinfink, H. (1962) Crystal structure of a trioctahedral mica: phlogopite. American Mineralogist, 47, 886–896.

Manuscript received, May 28, 1981;
accepted for publication, September 24, 1981.